Deterministic generation of arbitrary *n*-photon states in a waveguide-QED system

Fan Xing, Zeyang Liao,* and Xue-hua Wang

State Key Laboratory of Optoelectronic Materials and Technologies, School of Physics, Sun Yat-sen University, Guangzhou 510275, China

(Received 21 April 2023; revised 17 November 2023; accepted 2 January 2024; published 22 January 2024)

Quantum light sources play a vital role in various aspects of quantum information science, but on-demand highly efficient generation of arbitrary multiphoton states which can be easily integrated is still challenging. Here, we propose a chip-integrable scheme to deterministically generate a group of n photons with very high fidelity based on the long-range collective interaction between the emitters mediated by the waveguide modes. The n photons are shown to be emitted in a bundle while two successive n-photon bundles tend to be antibunched and can behave as an n-photon gun. Our results here can find applications in areas such as chip-integrated quantum information processing and quantum metrology.

DOI: 10.1103/PhysRevA.109.013718

I. INTRODUCTION

Classical coherent light sources like lasers have been extensively applied in many areas and have played important roles in modern information science [1,2]. Similarly, quantum light sources such as single-photon sources and entangled photon sources have become key ingredients for photonic quantum technologies [3–8]. The single-photon sources can be heralded generated by the parametric down-conversion [9–11] or four-wave mixing processes [12], but these methods are usually probabilistic and their efficiencies are usually very low. The photon blockade effect can also be exploited for single-photon generation in the cavity quantum electrodynamics (QED) system, but the efficiency is also not very high [13–19]. During the past two decades, solid-state quantum emitters like semiconductor quantum dots (QDs) have been shown to be a very promising material platform for on-demand high-efficiency and high-quality single-photon sources [20–26] and entangled photon sources [27,28]. Single-photon sources generated by a high-quality QD have been temporally multiplexed to demonstrate highly efficient Boson sampling [29,30]. Although the quantum advantages have been demonstrated using very bright squeezed light sources (Gaussian Boson sampling) [31,32], the quantum advantages for the original Boson sampling problem have not yet been demonstrated due to the lack of multiphoton Fock states with high purity and indistinguishability.

In recent years, multiphoton Fock states or bundle emissions where the system emits a bundle of strongly correlated n photons have attracted much attention due to their fundamental applications in areas such as quantum information protocols [33], N-photon lasers and photon guns [34], quantum lithography and metrology [35,36], medical applications with high resolution and minimum harm to tissue [37,38], and biological photoreceptors with sensitivities greater than classical light [39,40]. The Fock state can be conditionally generated via the state collapse from a coherent or thermal state [41,42], but this process is not deterministic and the probability decreases rapidly when n increases. By accurately controlling the cavity-qubit coupling strength and interaction times, multiple-photon states can also be prepared [43–47]. Muñoz *et al.* showed that a strongly coupled cavity-atom system can form a series of anharmonic dressed states and if the pumping frequency satisfies the right conditions the system can emit n photons in a bundle [48]. Actually, if the usual Jaynes-Cummings (JC) Hamiltonian in the cavity-QED system can be generalized to the higher-order n-photon JC Hamiltonian [49–51], the coupled system can oscillate between the ground state and the n-excitation state (i.e., super-Rabi oscillations) and an n-photon state can be also generated [52,53]. Taking advantage of the nonlinear dynamics of the Cooper-pair tunneling or the ultrastrong coupling, the effective Hamiltonian of the circuit-QED system can be described by the n-photon JC model and antibunched N-photon bundles can also be generated [54–57]. However, when n is relatively larege, the efficiencies of the above methods are usually low. Uria *et al.* showed that a cavity field initially in a coherent state interacting with an atom can evolve to a quantum state close to a Fock-like state at a certain interaction time, and they numerically showed that an $n \sim 100$ Fock-like state with 70% fidelity can be generated [58]. However, the generated state in this method is not a Fock state but a displaced Fock state. By coupling the field to a multilevel atom, multiple photons can also be generated [59–61], but the number of photons is largely restricted by the available atomic levels. González-Tudela *et al.* proposed an interesting method for deterministic generation of arbitrary multiphoton states in a waveguide-QED system by pumping all N emitters into many-body collective states with n excitations step by step through carefully designed pulse sequences [62,63]. In their scheme, they need to couple a dipole-forbidden transition, and two-photon transitions were also required, which may present difficulties in experimental realization.

In this paper, we propose an alternative scheme to generate arbitrary n-photon states on demand in a waveguide-QED

*liaozy7@mail.sysu.edu.cn

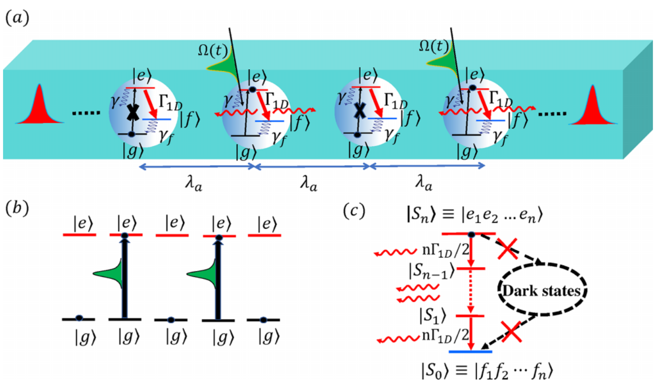

FIG. 1. (a) Schematic diagram for generating n-photon bundle states in a 1D waveguide-QED system where N multilevel emitters couple to the waveguide. (b) The emitters are selectively pumped from the ground state $|g\rangle$ to the excited $|e\rangle$ by external driving π pulses. The emitters without being pumped remain in the ground state. (c) The emitters being pumped to the excited state $|e\rangle$ can couple to the waveguide and they can collectively decay to the intermediate state $|f\rangle$ and release n highly correlated photons into the waveguide.

system which may be relatively easier to implement. In our scheme, we employ the long-range dipole-dipole interaction mediated with waveguide modes where the emitters with large separation can still have strong collective interactions [64–69]. Since the emitters here need not be very close, we can selectively pump a specific number of emitters into the excited state $|e\rangle$ by applying multiple ultrashort coherent π pulses whose duration is much less than the collective decay time of the emitters. Different from the methods proposed by González-Tudela *et al.* [62,63] where they pump all N emitters into a superposition state with n excitations step by step, here we selectively pump n out of N emitters to their excited states by a single step. Only the n emitters in the excited state can couple to the waveguide and then they can cascade down to the ground state through the superradiant pathway which can deterministically emit n photons into the waveguide. Our results show that the photons are emitted in a bundle and the photons in different bundles are antibunched. The proposed scheme can find applications in areas such as studying multiphoton nonlinear effects and collective many-body physics, demonstrating Boson sampling, and enhancing phase measurement sensitivity in the chip-integrated photonic system [70–78].

This article is organized as follows. In Sec. II, we discuss our scheme and the theoretical calculation methods. In Sec. III, we numerically demonstrate the validity of our scheme through three-atom examples. Finally, we summarize our results.

II. MODEL AND THEORY

The schematic model is shown in Fig. 1(a) where N identical multilevel emitters couple to a one-dimensional (1D) single-mode waveguide such as a photonic crystal waveguide, a superconducting transmission line, or a plasmonic nanowire. Among these atomic levels, only the transition between $|e\rangle$ and $|f\rangle$ with transition frequency ω_{ef} can couple to the waveguide modes, and other transitions are decoupled from the waveguide but they can couple to the external nonguided fields. The emitters are initially in the ground state $|g\rangle$, which decouples to the waveguide, and can be selectively pumped to the excited state $|e\rangle$ by an external laser π pulse whose frequency is tuned to be resonant with the $|g\rangle \rightarrow |e\rangle$ transition [Fig. 1(b)]. The emitters without being pumped will stay in the ground state $|g\rangle$ which is decoupled from the waveguide. An emitter in the excited state $|e\rangle$ can either decay to the state $|f\rangle$ with rate Γ_{1D} and emit a photon into the waveguide or decay back to the ground state $|g\rangle$ with rate γ and emit a photon to the free space. For a single-emitter case, the collection efficiency is given by $\Gamma_{1D}/(\Gamma_{1D}+\gamma)$. For the n-emitter excitation case, the emitters can collectively decay to the state $|f\rangle$ and emit n photons into the waveguide. The collection efficiency can be enhanced as follows: $n\Gamma_{1D}/(n\Gamma_{1D}+\gamma)$. The emitters in the state $|f\rangle$ can cascade down to the ground state $|g\rangle$ through certain intermediate states with the effective decay rate γ_f. By repeating the above procedures, we can produce a sequence of photon pulses with each pulse containing an n-photon bundle. This is the basic principle of our scheme.

To deterministically generate pure n-photon states, it is critical to selectively pump n emitters into the excited state $|e\rangle$ with high fidelity, and the other irrelevant emitters are decoupled from the waveguide. To achieve this, we apply multiple focused laser beams to the target emitters from the direction perpendicular to the waveguide. The emitter distance is chosen to be much larger than the diffraction limit which is about half wavelength to avoid cross excitation. In addition, to ensure that the selected emitters are prepared in the excited states $|e\cdots e\rangle$ with very high fidelity, the pulses are chosen to be π pulses and their time duration should be much less than the collective decay time of the emitters ($1/n\Gamma_{1D}$). Under this condition, the emitters almost do not decay during the pumping process and after that they decay without pumping to avoid the occurrence of reexcitations.

The emitters in the excited $|e\rangle$ state can couple to the waveguide and they can form collective states due to atom-atom interaction mediated by the waveguide modes. By tracing out the effects of the waveguide field, the effective Hamiltonian of the emitters in the subspace of $|e\rangle$ and $|f\rangle$ is given by [64,65,79]

$$H_{\text{eff}}^{(ef)} = \hbar\omega_{ef}\sum_j \sigma_{ef}^j\sigma_{fe}^j - i\frac{\hbar\Gamma_{1D}}{2}\sum_{j,l=1}^{N} e^{ik_a z_{jl}}\sigma_{ef}^j\sigma_{fe}^l, \quad (1)$$

where the real part gives the collective effective energy and the imaginary part describes the collective decay rates. $\sigma_{ef}^j = |e\rangle_j\langle f|$ is the operator that describes the $|f\rangle \rightarrow |e\rangle$ transition of the jth emitter. $z_{jl} = |z_j - z_l|$ is the distance between the jth and lth emitters. By diagonalizing $H_{\text{eff}}^{(ef)}$, we can obtain the effective collective eigenenergies and eigenstates of the emitter system in the subspace spanned by $|e\rangle$ and $|f\rangle$. Due to the collective interactions, some states are superradiant and others are subradiant. Here, we consider the case when the emitter distances are integer multiple of resonant wavelength under which the subradiant states completely decouple from the waveguide field and only the superradiant states can couple to the waveguide. Without loss of generality, here we assume that the distance between the nearest-neighbor emitters is the resonant wavelength λ_a corresponding to the transition frequency ω_{ef}. The superradiant states are given by $|S_m\rangle = \frac{1}{\sqrt{n}}\mathrm{sym}\{|e\rangle^{\otimes m}|f\rangle^{\otimes(n-m)}\}$, which is the symmetric superposition of the states with n emitters being in the state $|e\rangle$ and the other $n-m$ emitters being in the state $|f\rangle$. The eigenenergy of the state $|S_m\rangle$ is $m\omega_{ef}$ with the collective decay rate $\Gamma_m = m(n-m+1)\Gamma_{1D}/2$, where $m = 0, 1, \ldots, n$ [Fig. 1(c)]. When $m = 0$, $|S_0\rangle = |f\ldots f\rangle$ is the lowest energy eigenstate in the subspace, while when $m = n$, $|S_n\rangle = |e\ldots e\rangle$ is the highest energy eigenstate with the decay rate $n\Gamma_{1D}/2$, which is n times larger than that of the single emitter decay rate. For other values of m, the collective decay rates can be larger than $n\Gamma_{1D}/2$. If the emitter system is prepared in the state $|S_n\rangle$ with high fidelity, it can cascade down to the ground state through the superradiance pathway and deterministically emit n photons with high purity. Due to the superradiant effect, the emitted n photons are bounded in the time and space domain.

III. NUMERICAL SIMULATION

To prove the validity of our scheme, we can numerically calculate the population dynamics and the photon statistics by either solving the master equation [80] or using the quantum Monte Carlo method (see Appendixes A and B) [81–83]. Here, as an example, we consider the case when three emitters couple with a 1D waveguide and compare the results when one or two or three emitters are excited. The nearest-neighbor separation between the emitters is set to be λ_a. Here we assume that the spontaneous decay loss to the free space $\gamma = 0.05\Gamma_{1D}$, which is realistic because as low as 1% loss has been experimentally demonstrated in quantum dots coupled to the photonic crystal waveguide [84] and in superconducting qubits coupled to the superconducting tranmission line [85,86]. The effective decay rate from the state $|f\rangle$ to the ground state $|g\rangle$ is given by $\gamma_f = 2\Gamma_{1D}$. Initially, all the emitters are in the ground state. We then apply multiple coherent driving π pulses with a time duration much less than the collective decay time $1/n\Gamma_{1D}$ ($n = 3$ in this example) to selectively excite a certain number of emitters. In the following numerical simulations, we assume that the driving pulse is Gaussian π pulses with the spectrum width $\Delta = 200\Gamma_{1D}$ and average photon number $\bar{n}_d = 4182$ (see Appendix A). The peak driving Rabi frequency $\Omega = \sqrt{\gamma\bar{n}_d\Delta/2\pi^{1/4}}$, which is about $125\Gamma_{1D}$ under the chosen parameters. For a quantum dot coupled to a photonic crystal waveguide where $\Gamma_{1D} \approx$ 200 MHz, the peak driving Rabi frequency is about 25 GHz, which is experimentally achievable [87].

A. Population dynamics and photon statistics

The population dynamics of the emitter system as a function of time and the photon statistics for the three excitation cases are shown in Fig. 2.

Case 1. If only one emitter is excited by a short coherent π pulse at the time marked by a red arrow shown in Fig. 2(a), we can see that the emitter is then in the $|e\rangle$ state after the pulse with very high fidelity (about 99% in this example). After that, the excited emitter decays to the ground state through the path $|e\rangle \to |f\rangle \to |g\rangle$ and emits a single photon into the waveguide with about 97.7% probability according to the numerical Monte Carlo simulation [Fig. 2(b)]. There is about

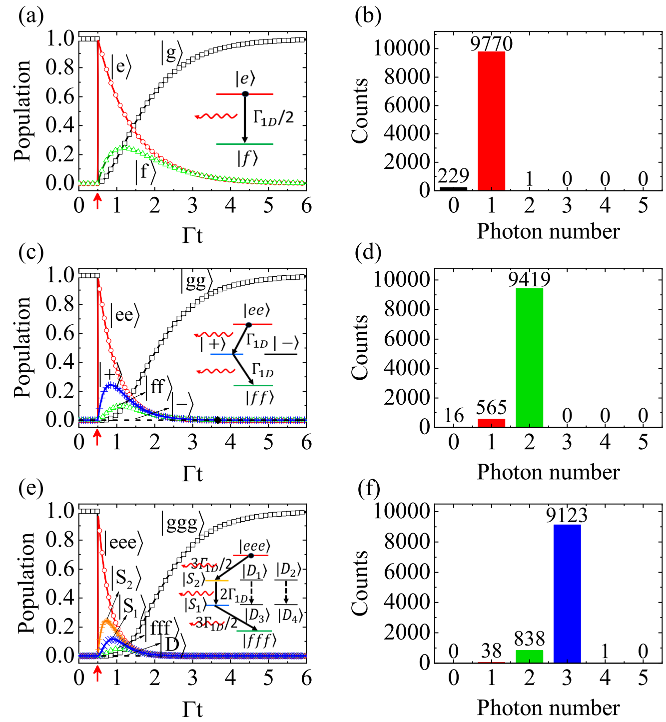

FIG. 2. Population dynamics and photon count statistics for the one-excitation case (a), (b), the two-excitation case (c), (d), and the three-excitation case (e), (f).

a 2.3% probability that the emitter directly decays back to the ground state and emits a photon into the free space with zero photons in the waveguide.

Case 2. If we selectively excite two emitters (e.g., the first and second emitters) by two separate short coherent π pulses at the time marked by the red arrow shown in Fig. 2(c), the system can be in the state $|ee\rangle$ after the pulse with about 97.7% in our numerical example. The excited emitters then decay back to the ground state through the path $|ee\rangle \to |+\rangle \to |ff\rangle \to |gg\rangle$, where $|\pm\rangle = \frac{1}{\sqrt{2}}(|ef\rangle \pm |fe\rangle)$ [Fig. 2(c)], and emit two photons into the waveguide with the probability being about 94.2% [Fig. 2(d)]. It is clearly seen that the system decays through the superradiant path since the population in the subradiant state $|-\rangle$ is always zero [black dashed line in Fig. 2(c)]. The Monte Carlo simulation shows that the probability of one-photon loss is about 5.6% and the probability of two-photon loss is about 0.2% [Fig. 2(d)].

Case 3. If three emitters are excited by three short coherent π pulses with the probability being about 96.5% in our numerical example, they can decay back to the ground state through the path $|eee\rangle \to |S_2\rangle \to |S_1\rangle \to |fff\rangle \to |ggg\rangle$, where $|S_2\rangle = \frac{1}{\sqrt{3}}(|eef\rangle + |efe\rangle + |fee\rangle)$ and $|S_1\rangle = \frac{1}{\sqrt{3}}(|\mathrm{eff}\rangle + |fef\rangle + |ffe\rangle)$ as shown in Fig. 2(e). In this process, the system can emit three photons into the waveguide with the probability being about 91.2% [Fig. 2(f)]. According to our Monte Carlo simulation, the probabilities of one-, two- and three-photon losses are about 8.38%, 0.38%, and 0%, respectively. From the photon distribution shown in Fig. 2, we can clearly see that the generated photon states are highly nonclassical.

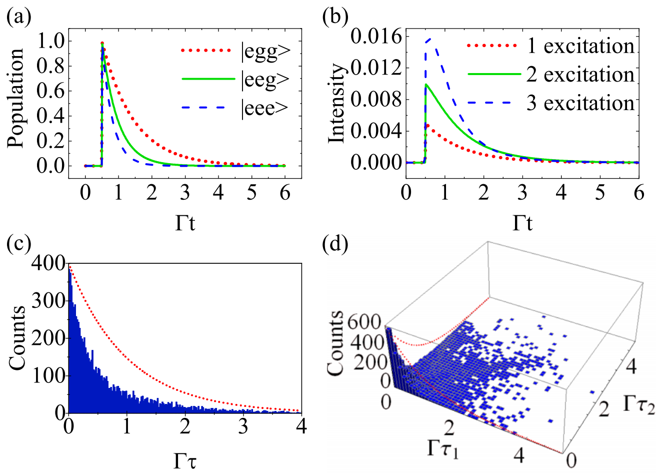

FIG. 3. Comparison of the population decay dynamics (a) and the output photon intensities (b) of the cases when one, two, and three emitters are excited. Statistics of the time intervals of the 9419 two-photon events (c) and the 9123 three-photon events (d) observed in Fig. 2.

To clearly see that the photons are indeed emitted by the collective decay, we compare the population decay dynamics of the three cases as shown in Fig. 3(a). We can see that the more emitters are excited the faster the decay rate is, which is a signature of the superradiant effect. The output photon intensity as a function of time for three different cases is shown in Fig. 3(b), from which we can see that the emitted field intensity is proportional to the number of excited emitters and the photon pulse shape is sharper when more emitters are excited, which is another signature of the supperradiant effect. In Fig. 3(c), we show the statistics of the time interval between two successive emitted photons for the case when two emitters are excited. The red dotted lines in Figs. 3(c) and 3(d) are the single-photon emission curves for comparison. It is clearly seen that the two emitted photons tend to bunch together. Similarly, the statistics of the time intervals between the three successive photons for the case when three emitters are excited is shown in Fig. 3(d), from which we can also clearly see the bunching effect among the photons in each bundle.

B. Generalized second-order correlation function

The property of the generated photons can be captured by calculating the higher-order correlation function, especially the second-order correlation function $g^{(2)}(\tau) = \lim_{t\to\infty}\langle a^\dagger(t)a^\dagger(t+\tau)a(t+\tau)a(t)\rangle/\langle a^\dagger(t)a(t)\rangle^2$, where $a(t) = \int d\omega a(\omega)e^{-i\omega t}/2\pi$ is the time-dependent annihilation of a photon mode [88]. For a photon mode with a frequency bandwidth, in principle, we need to integrate all the frequencies belonging to each mode. In the numerical simulation, we directly calculate the average value of the time-dependent operators like $\langle a^\dagger(t)a(t)\rangle$ and $\langle a^\dagger(t)a^\dagger(t+\tau)a(t+\tau)a(t)\rangle$ from the input-output relations which already integrate all the frequencies in each mode. The above $g^{(2)}(\tau)$ function has been widely used to calculate the correlation of photons in the waveguide-QED system [81,87,89]. However, since the above $g^{(2)}(\tau)$ formula is

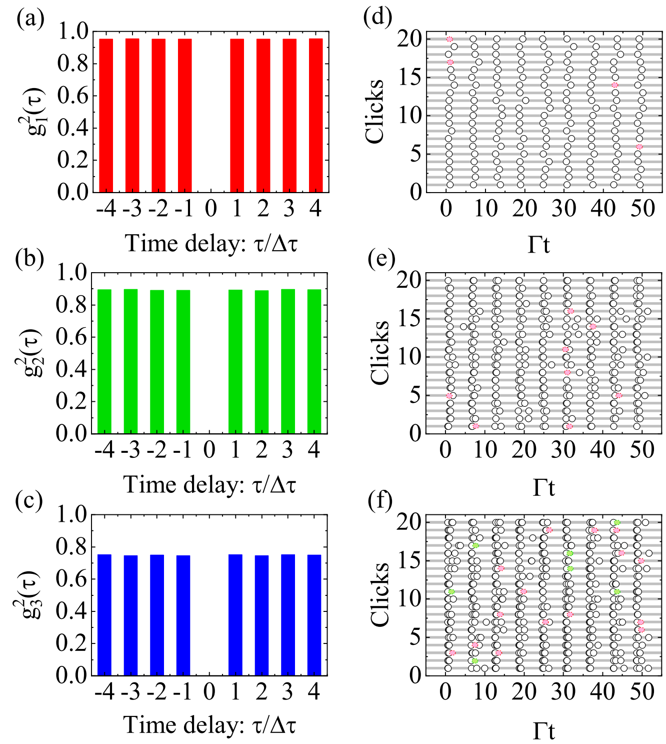

FIG. 4. Generalized second-order correlation functions driven by nine pulses (a)–(c). Clicks over 20 quantum trajectories by quantum Monte Carlo simulation (d)–(f). (a), (d) One-atom excitation, (b), (e) two-atom excitation, and (c), (f) three-atom excitation.

usually used for the stationary solution with continuous wave pumping, to confirm that the photons are indeed emitted by bundles, we here calculate the generalized second-order correlation function for the pulse excitation [88] as

$$g_n^{(2)}[m] = \frac{\langle a^{\dagger n}[0]a^{\dagger n}[m]a^n[m]a^n[0]\rangle}{\langle (a^{\dagger n}a^n)[0]\rangle\langle (a^{\dagger n}[m]a^n[m])\rangle}, \tag{2}$$

where m is an integer number denoting the pulse index and the angled brackets indicate the ensemble average. Here "0" in the square bracket does not mean zero time but the first time gap $\Delta\tau$ between the zeroth and the first excitation pulses. m denotes the time gap between the mth pulse to the $(m+1)$th pulse. Therefore, the expression shown in Eq. (2) counts for the correlations between the emitted n photons in each pulse. In the numerical simulation, we count the average photon number that arrived at the first time gap and that arrived at the mth time gap to calculate the generalized second-order function. When $n = 1$, it returns back to the usual second-order correlation function defined for pulse excitation. When $n > 1$, it is the generalized second-order correlation function characterizing the n-photon bundle emission under pulse excitation. $g_n^2[0] = 0$ indicates that the two n-photon bundles never come together. The generalized second-order correlation functions for the one-, two-, and three-photon cases are shown in Figs. 4(a), 4(b), and 4(c), respectively. From the figures, we can see that $g_1^2[0] = g_2^2[0] = g_3^2[0] = 0$. The results clearly show that the photons are indeed emitted by bundles and the bundles are antibunched.

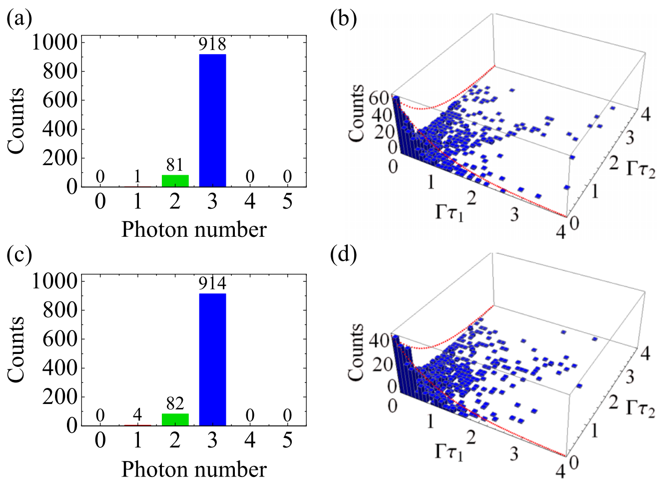

FIG. 5. Photon count statistics and statistics of the time intervals of the three-photon events for exciting three quantum emitters (1000 total trajectories). (a), (b) The quantum emitters have the same frequency but their positions are set to 0, 0.95λ, and 2.1λ. (c), (d) The quantum emitters are spaced at integer wavelengths, while the frequencies deviate from the resonant frequency by $\Delta\epsilon_1 = \Gamma_{1D}/10$, $\Delta\epsilon_2 = -\Gamma_{1D}/10$, and $\Delta\epsilon_3 = \Gamma_{1D}/8$.

The time structures of the emitted events by nine consecutive driving pulses with separation $\Delta\tau = 6/\Gamma_{1D}$ are shown in Figs. 4(d)–4(f), in which each black circle indicates radiating a single photon, each red circle indicates the absence of one photon, and each green circle indicates the absence of two photons. The results clearly show the bundle emissions such that one-photon, two-photon, and three-photon events predominate when one, two, and three emitters are excited, respectively. The occasional photon losses are mainly due to the decay channel from $|e\rangle \rightarrow |g\rangle$, in which the photons are emitted to the free space.

Because quantum dots have a large inhomogeneous broadening and cannot be positioned deterministically, we calculate the results when the atomic spacing is not strictly equal to the wavelength and when the frequency of the quantum dot is modulated for exciting three quantum dots. From Fig. 5, the three-photon yield does not decrease, and the emitted three photons are still bunched in nonideal situations. This shows that our scheme is robust to the uncertainty of atomic positions and the large inhomogeneous broadening of quantum dots.

C. Nonideal case: Position uncertainty and inhomogeneous broadening

In the above discussions, we mainly consider the ideal case that the emitter distance is integer multiple of resonant wavelength. However, the positions of the emitters may not be placed at the required positions exactly in practice. Here, we study the effects of position inaccuracy, i.e., the case when the emitter spacing is not strictly equal to the wavelength. One example is shown in Figs. 5(a) and 5(b) where the emitter positions are set to be 0, 0.95λ, and 2.1λ. We can see that the purity of the three photons is still very good (>90%) and the generated three photons are still tightly bound. Therefore, our scheme can still work even if the emitters are not placed exactly at the required positions.

In practical realization, inhomogeneous broadening of quantum emitters is another issue that needs to be considered. Our theoretical proposal can be applied to various physical systems such as superconducting qubits coupled to superconducting transmission lines or quantum dots coupled to photonic crystal waveguides. For the first case, the transition frequency of the superconducting qubit can be easily tuned by the external magnetic field. For the latter case, there are also some methods to tune the transition frequency of quantum dots such as by either electromagnetic field or strain. For example, in Ref. [87], they experimentally showed that two quantum dots can be electrically tuned to the same frequency using a pair of isolated p-i-n junctions. Nevertheless, here we also numerically calculate the cases when the emitter frequencies are not exactly the same. The results are shown in Figs. 5(c) and 5(d), where the transition frequencies of the three emitters deviate from the resonant frequency by the amounts $\Delta\epsilon_1 = \Gamma_{1D}/10$, $\Delta\epsilon_2 = -\Gamma_{1D}/10$, and $\Delta\epsilon_3 = \Gamma_{1D}/8$. Our results show that in this case the purity of the three photons is still good (>90%) and the generated three photons are still well bound. Therefore, our scheme can also tolerate a certain frequency fluctuation.

IV. SUMMARY

To conclude, we propose a scheme to deterministically generate an arbitrary n-photon number state on demand in an integrated quantum electrodynamics system. Our results show that by selectively pumping a certain number of emitters into the excited state they can collectively decay to the ground state and emit a certain number of photons into the waveguide. The numerical results show that these photons are emitted by bundles and the photons within each bundle are highly correlated even if the emitter position and frequency has certain uncertainties. Our study here can find applications for on-chip integrated quantum information technology and quantum metrology.

ACKNOWLEDGMENTS

This work was supported by the National Key R&D Program of China (Grant No. 2021YFA1400800), the Key-Area Research and Development Program of Guangdong Province (Grant No. 2018B030329001), and Applied Basic Research Foundation (Grant No. 2023B1515040023), and the Natural Science Foundations of Guangdong (Grant No. 2021A1515010039).

APPENDIX A: MASTER EQUATION

To prove the validity of our scheme, we can numerically solve the driven master equation [64,80]

$$\dot{\rho}_s(t) = -i[H_{\rm coh}, \rho_s(t)] + \mathcal{L}[\rho_s(t)], \tag{A1}$$

with the coherent Hamiltonian given by

$$H_{\rm coh}(t) = \sqrt{\frac{\gamma}{2}} \sum_{j=1}^{n} \left[\alpha_j(t)\sigma_{eg}^j + \alpha_j^*(t)\sigma_{ge}^j\right] + \frac{\Gamma_{1D}}{2} \sum_{jl} \sin(k_a z_{jl})\sigma_{ef}^j \sigma_{fe}^l, \tag{A2}$$

where the first term is the external pumping term and the second term is the coherent atom-atom interaction mediated by the waveguide modes. $\alpha_j(t)$ is the time-dependent field amplitude of the incident photon pulse. Here, we assume that the pumping photon pulses are the same and they are all short Gaussian pulses which are given by $\alpha_j(t) = \sqrt{\frac{\bar{n}_d \Delta}{\pi^{1/4}}} e^{-\frac{\Delta^2 (x_0/c - t)^2}{2}} e^{ik_a x_0}$, where $\bar{n}_d$ is the average photon number of the driving field, Δ is the spectrum width, c is the speed of light, and x_0 is the initial central peak position. Here we assume that the central frequency of the driving field is resonant with the atomic bare frequency. The driving Rabi frequency is given by $\Omega_j(t) = \sqrt{\gamma/2}\alpha_j(t)$, with the peak Rabi frequency given by $\sqrt{\gamma \bar{n}_d \Delta / 2\pi^{1/4}}$.

The second term on the right-hand side of Eq. (1) describes the dissipation of the emitter system given by

$$\mathcal{L}[\rho_s(t)] = -\frac{\Gamma_{1D}}{2} \sum_{j,l=1}^{N} \cos(k_a z_{jl}) \mathcal{L}_{ef}^{jl}[\rho_s(t)] - \frac{\gamma}{2} \sum_{j=1}^{N} \mathcal{L}_{eg}^{jj}[\rho_s(t)] - \frac{\gamma_f}{2} \sum_{j=1}^{N} \mathcal{L}_{fg}^{jj}[\rho_s(t)], \quad \text{(A3)}$$

where $\mathcal{L}_{ef}^{jl}[\rho_s(t)] = \sigma_{ef}^{j} \sigma_{fe}^{l} \rho_s(t) + \rho_s(t) \sigma_{ef}^{j} \sigma_{fe}^{l} - 2\sigma_{fe}^{l} \rho_s(t) \sigma_{ef}^{j}$, $\mathcal{L}_{eg}^{jj}[\rho_s(t)] = \sigma_{eg}^{j} \sigma_{ge}^{j} \rho_s(t) + \rho_s(t) \sigma_{eg}^{j} \sigma_{ge}^{j} - 2\sigma_{ge}^{j} \rho_s(t) \sigma_{eg}^{j}$, and $\mathcal{L}_{fg}^{jj}[\rho_s(t)] = \sigma_{fg}^{j} \sigma_{gf}^{j} \rho_s(t) + \rho_s(t) \sigma_{fg}^{j} \sigma_{gf}^{j} - 2\sigma_{gf}^{j} \rho_s(t) \sigma_{fg}^{j}$. From the master equation shown in Eq. (2), we can solve the population dynamics of the emitter system.

APPENDIX B: QUANTUM MONTE CARLO METHOD

To calculate the photon statistics of the output field, it is convenient to use the quantum Monte Carlo method [81–83]. The effective Hamiltonian of the emitter system can be written as

$$H_{\text{eff}}(t) = H_{\text{coh}}(t) - \frac{i\hbar}{2} \sum_{\beta = R, L, \gamma, \gamma_f} J_\beta^+ J_\beta^-, \quad \text{(B1)}$$

where $H_{\text{coh}}(t)$ is given by Eq. (A2) and the effective jumping operators $J_{R,L}^- = \sqrt{\frac{\Gamma_{1D}}{2}} \sum_{j=1}^{N} e^{\mp ik_a z_j} \sigma_{fe}^{j}(t)$, $J_\gamma^- = \sqrt{\frac{\gamma}{2}} \sum_{j=1}^{N} \sigma_{ge}^{j}(t)$, and $J_{\gamma_f}^- = \sqrt{\frac{\gamma_f}{2}} \sum_{j=1}^{N} \sigma_{gf}^{j}(t)$. Having the effective Hamiltonian, we can use the quantum Monte Carlo method to numerically calculate the dynamics of the system and the photon statistics with the following steps.

(i) Suppose the wave function at time t is $|\varphi(t)\rangle$.

(ii) Calculate the probabilities: $P_{R,L} = dt\langle\varphi(t)|J_{R,L}^+ J_{R,L}^-|\varphi(t)\rangle$ is the probability that the emitters jump from the $|e\rangle$ state to the $|f\rangle$ state and emit a photon to the right (left) direction; $P_\gamma = dt\langle\varphi(t)|J_\gamma^+ J_\gamma^-|\varphi(t)\rangle$ is the probability that the emitters jump from the $|e\rangle$ state to the $|g\rangle$ state and emit a photon to the free space; and $P_{\gamma_f} = dt\langle\varphi(t)|J_{\gamma_f}^+ J_{\gamma_f}^-|\varphi(t)\rangle$ is the probability that the emitters jump from the $|f\rangle$ state to the $|g\rangle$ state and emit a photon to the free space.

(iii) Choose a random number r between 0 and 1, and if (a) $r < P_\gamma$, $|\varphi(t+dt)\rangle = J_\gamma^-|\varphi(t)\rangle/\sqrt{P_\gamma/dt}$, a photon emits to the free space; (b) $P_\gamma < r < P_\gamma + P_R$, $|\varphi(t+dt)\rangle = J_R^-|\varphi(t)\rangle/\sqrt{P_R/dt}$, a photon emits to the right within waveguide; (c) $P_\gamma + P_R < r < P_\gamma + P_R + P_L$, $|\varphi(t+dt)\rangle = J_L^-|\varphi(t)\rangle/\sqrt{P_L/dt}$, a photon emits to the left within the waveguide; (d) $P_\gamma + P_R + P_L < r < P_\gamma + P_R + P_L + P_{\gamma_f}$, $|\varphi(t+dt)\rangle = J_{\gamma_f}^-|\varphi(t)\rangle/\sqrt{P_{\gamma_f}/dt}$, a photon decay to ground states from $|f\rangle$. (e) $r > P_\gamma + P_R + P_L + P_{\gamma_f}$, $|\varphi(t+dt)\rangle = (I - iH_{\text{eff}}dt)|\varphi(t)\rangle/\sqrt{1-(P_R+P_L+P_\gamma+P_{\gamma_f})}$, no photon is emitted and the system evolves coherently.

(iv) Repeat the above procedures for a sufficiently large number of times, we can then obtain the density of the state at arbitrary time by averaging over the results of each trajectory, i.e., $|\rho(t)\rangle = \sum_m |\varphi_m(t)\rangle\langle\varphi_m(t)|$, where m denotes each trajectory, and we can also calculate the photon statistics including photon counts, photon correlations, and so on.

[1] T. H. Maiman, Stimulated optical radiation in ruby, Nature (London) **187**, 493 (1960).
[2] W. Song, A. C. Anselmo, and L. Huang, Nanotechnology intervention of the microbiome for cancer therapy, Nat. Nanotechnol. **14**, 1093 (2019).
[3] R. Trivedi, K. A. Fischer, J. Vučković, and K. Müller, Generation of non-classical light using semiconductor quantum dots, Adv. Quantum Technol. **3**, 1900007 (2020).
[4] P. Kok, W. J. Munro, K. Nemoto, T. C. Ralph, J. P. Dowling, and G. J. Milburn, Linear optical quantum computing with photonic qubits, Rev. Mod. Phys. **79**, 135 (2007).
[5] A. P. Lund, A. Laing, S. Rahimi-Keshari, T. Rudolph, J. L. O'Brien, and T. C. Ralph, Boson sampling from a Gaussian state, Phys. Rev. Lett. **113**, 100502 (2014).
[6] A. K. Ekert, Quantum cryptography based on Bell's theorem, Phys. Rev. Lett. **67**, 661 (1991).
[7] B. Hensen, H. Bernien, A. E. Dréau, A. Reiserer, N. Kalb, M. S. Blok, J. Ruitenberg, R. F. Vermeulen, R. N. Schouten, C. Abellán *et al.*, Loophole-free Bell inequality violation using electron spins separated by 1.3 kilometres, Nature (London) **526**, 682 (2015).
[8] J. Nilsson, R. Stevenson, K. Chan, J. Skiba-Szymanska, M. Lucamarini, M. Ward, A. Bennett, C. Salter, I. Farrer, D. Ritchie *et al.*, Quantum teleportation using a light-emitting diode, Nat. Photon. **7**, 311 (2013).
[9] A. Heidmann, R. J. Horowicz, S. Reynaud, E. Giacobino, C. Fabre, and G. Camy, Observation of quantum noise reduction on twin laser beams, Phys. Rev. Lett. **59**, 2555 (1987).
[10] G. Harder, T. J. Bartley, A. E. Lita, S. W. Nam, T. Gerrits, and C. Silberhorn, Single-mode parametric-down-conversion states with 50 photons as a source for mesoscopic quantum optics, Phys. Rev. Lett. **116**, 143601 (2016).
[11] L. S. Madsen, F. Laudenbach, M. F. Askarani, F. Rortais, T. Vincent, J. F. Bulmer, F. M. Miatto, L. Neuhaus, L. G. Helt, M. J. Collins *et al.*, Quantum computational advantage with

a programmable photonic processor, Nature (London) **606**, 75 (2022).
[12] S. Paesani, M. Borghi, S. Signorini, A. Maïnos, L. Pavesi, and A. Laing, Near-ideal spontaneous photon sources in silicon quantum photonics, Nat. Commun. **11**, 2505 (2020).
[13] K. Müller, A. Rundquist, K. A. Fischer, T. Sarmiento, K. G. Lagoudakis, Y. A. Kelaita, C. Sánchez Muñoz, E. del Valle, F. P. Laussy, and J. Vučković, Coherent generation of nonclassical light on chip via detuned photon blockade, Phys. Rev. Lett. **114**, 233601 (2015).
[14] C. Hamsen, K. N. Tolazzi, T. Wilk, and G. Rempe, Two-photon blockade in an atom-driven cavity QED system, Phys. Rev. Lett. **118**, 133604 (2017).
[15] M. Chen, J. Tang, L. Tang, H. Wu, and K. Xia, Photon blockade and single-photon generation with multiple quantum emitters, Phys. Rev. Res. **4**, 033083 (2022).
[16] J. McKeever, A. Boca, A. D. Boozer, R. Miller, J. R. Buck, A. Kuzmich, and H. J. Kimble, Deterministic generation of single photons from one atom trapped in a cavity, Science **303**, 1992 (2004).
[17] B. Darquié, M. P. A. Jones, J. Dingjan, J. Beugnon, S. Bergamini, Y. Sortais, G. Messin, A. Browaeys, and P. Grangier, Controlled single-photon emission from a single trapped two-level atom, Science **309**, 454 (2005).
[18] R. Trivedi, M. Radulaski, K. A. Fischer, S. Fan, and J. Vučković, Photon blockade in weakly driven cavity quantum electrodynamics systems with many emitters, Phys. Rev. Lett. **122**, 243602 (2019).
[19] Y.-W. Lu, J.-F. Liu, Z. Liao, and X.-H. Wang, Plasmonic-photonic cavity for high-efficiency single-photon blockade, Sci. China: Phys., Mech. Astron. **64**, 274212 (2021).
[20] L. Zhai, G. N. Nguyen, C. Spinnler, J. Ritzmann, M. C. Löbl, A. D. Wieck, A. Ludwig, A. Javadi, and R. J. Warburton, Quantum interference of identical photons from remote GaAs quantum dots, Nat. Nanotechnol. **17**, 829 (2022).
[21] P. Laferriere, E. Yeung, L. Giner, S. Haffouz, J. Lapointe, G. C. Aers, P. J. Poole, R. L. Williams, and D. Dalacu, Multiplexed single-photon source based on multiple quantum dots embedded within a single nanowire, Nano Lett. **20**, 3688 (2020).
[22] P. Michler, A. Kiraz, C. Becher, W. V. Schoenfeld, P. M. Petroff, L. Zhang, E. Hu, and A. Imamoglu, A quantum dot single-photon turnstile device, Science **290**, 2282 (2000).
[23] S. Buckley, K. Rivoire, and J. Vučković, Engineered quantum dot single-photon sources, Rep. Prog. Phys. **75**, 126503 (2012).
[24] X. Ding, Y. He, Z.-C. Duan, N. Gregersen, M.-C. Chen, S. Unsleber, S. Maier, C. Schneider, M. Kamp, S. Höfling, C.-Y. Lu, and J.-W. Pan, On-demand single photons with high extraction efficiency and near-unity indistinguishability from a resonantly driven quantum dot in a micropillar, Phys. Rev. Lett. **116**, 020401 (2016).
[25] I. Aharonovich, D. Englund, and M. Toth, Solid-state single-photon emitters, Nat. Photon. **10**, 631 (2016).
[26] N. Tomm, A. Javadi, N. O. Antoniadis, D. Najer, M. C. Löbl, A. R. Korsch, R. Schott, S. R. Valentin, A. D. Wieck, A. Ludwig *et al.*, A bright and fast source of coherent single photons, Nat. Nanotechnol. **16**, 399 (2021).
[27] M. Müller, S. Bounouar, K. D. Jöns, M. Glässl, and P. Michler, On-demand generation of indistinguishable polarization-entangled photon pairs, Nat. Photon. **8**, 224 (2014).
[28] J. Liu, R. Su, Y. Wei, B. Yao, S. F. C. d. Silva, Y. Yu, J. Iles-Smith, K. Srinivasan, A. Rastelli, J. Li *et al.*, A solid-state source of strongly entangled photon pairs with high brightness and indistinguishability, Nat. Nanotechnol. **14**, 586 (2019).
[29] J. C. Loredo, M. A. Broome, P. Hilaire, O. Gazzano, I. Sagnes, A. Lemaitre, M. P. Almeida, P. Senellart, and A. G. White, Boson sampling with single-photon Fock states from a bright solid-state source, Phys. Rev. Lett. **118**, 130503 (2017).
[30] H. Wang, Y. He, Y.-H. Li, Z.-E. Su, B. Li, H.-L. Huang, X. Ding, M.-C. Chen, C. Liu, J. Qin *et al.*, High-efficiency multiphoton boson sampling, Nat. Photonics **11**, 361 (2017).
[31] H.-S. Zhong, H. Wang, Y.-H. Deng, M.-C. Chen, L.-C. Peng, Y.-H. Luo, J. Qin, D. Wu, X. Ding, Y. Hu, P. Hu, X.-Y. Yang, W.-J. Zhang, H. Li, Y. Li, X. Jiang, L. Gan, G. Yang, L. You, Z. Wang *et al.*, Quantum computational advantage using photons, Science **370**, 1460 (2020).
[32] H.-S. Zhong, Y.-H. Deng, J. Qin, H. Wang, M.-C. Chen, L.-C. Peng, Y.-H. Luo, D. Wu, S.-Q. Gong, H. Su, Y. Hu, P. Hu, X.-Y. Yang, W.-J. Zhang, H. Li, Y. Li, X. Jiang, L. Gan, G. Yang, L. You *et al.*, Phase-programmable Gaussian boson sampling using stimulated squeezed light, Phys. Rev. Lett. **127**, 180502 (2021).
[33] S. Haroche and J.-M. Raimond, *Exploring the Quantum: Atoms, Cavities, and Photons* (Oxford University, Oxford, UK, 2006).
[34] B. Lounis and M. Orrit, Single-photon sources, Rep. Prog. Phys. **68**, 1129 (2005).
[35] V. Giovannetti, S. Lloyd, and L. Maccone, Quantum-enhanced measurements: Beating the standard quantum limit, Science **306**, 1330 (2004).
[36] V. Giovannetti, S. Lloyd, and L. Maccone, Advances in quantum metrology, Nat. Photon. **5**, 222 (2011).
[37] W. Denk, J. H. Strickler, and W. W. Webb, Two-photon laser scanning fluorescence microscopy, Science **248**, 73 (1990).
[38] N. G. Horton, K. Wang, D. Kobat, C. G. Clark, F. W. Wise, C. B. Schaffer, and C. Xu, In vivo three-photon microscopy of subcortical structures within an intact mouse brain, Nat. Photonics **7**, 205 (2013).
[39] N. Sim, M. F. Cheng, D. Bessarab, C. M. Jones, and L. A. Krivitsky, Measurement of photon statistics with live photoreceptor cells, Phys. Rev. Lett. **109**, 113601 (2012).
[40] P. Ball, Physics of life: The dawn of quantum biology, Nature (London) **474**, 272 (2011).
[41] C. Guerlin, J. Bernu, S. Deleglise, C. Sayrin, S. Gleyzes, S. Kuhr, M. Brune, J.-M. Raimond, and S. Haroche, Progressive field-state collapse and quantum non-demolition photon counting, Nature (London) **448**, 889 (2007).
[42] M. F. Santos, E. Solano, and R. L. de Matos Filho, Conditional large Fock state preparation and field state reconstruction in cavity QED, Phys. Rev. Lett. **87**, 093601 (2001).
[43] C. K. Law and J. H. Eberly, Arbitrary control of a quantum electromagnetic field, Phys. Rev. Lett. **76**, 1055 (1996).
[44] K. R. Brown, K. M. Dani, D. M. Stamper-Kurn, and K. B. Whaley, Deterministic optical Fock-state generation, Phys. Rev. A **67**, 043818 (2003).
[45] Y.-X. Liu, L. F. Wei, and F. Nori, Generation of nonclassical photon states using a superconducting qubit in a microcavity, Europhys. Lett. **67**, 941 (2004).
[46] M. Hofheinz, E. Weig, M. Ansmann, R. C. Bialczak, E. Lucero, M. Neeley, A. O'connell, H. Wang, J. M. Martinis, and A.

Cleland, Generation of Fock states in a superconducting quantum circuit, Nature (London) **454**, 310 (2008).
[47] K. Xia, G. K. Brennen, D. Ellinas, and J. Twamley, Deterministic generation of an on-demand Fock state, Opt. Express **20**, 27198 (2012).
[48] C. S. Muñoz, E. Del Valle, A. G. Tudela, K. Müller, S. Lichtmannecker, M. Kaniber, C. Tejedor, J. Finley, and F. Laussy, Emitters of N-photon bundles, Nat. Photon. **8**, 550 (2014).
[49] C. Sukumar and B. Buck, Multi-phonon generalisation of the Jaynes-Cummings model, Phys. Lett. A **83**, 211 (1981).
[50] S. Singh, Field statistics in some generalized Jaynes-Cummings models, Phys. Rev. A **25**, 3206 (1982).
[51] S.-Y. Jiang, F. Zou, Y. Wang, J.-F. Huang, X.-W. Xu, and J.-Q. Liao, Multiple-photon bundle emission in the n-photon Jaynes-Cummings model, Opt. Express **31**, 15697 (2023).
[52] C. J. Villas-Boas and D. Z. Rossatto, Multiphoton Jaynes-Cummings model: Arbitrary rotations in Fock space and quantum filters, Phys. Rev. Lett. **122**, 123604 (2019).
[53] X.-L. Yin, W.-B. Luo, and J.-Q. Liao, Non-Markovian disentanglement dynamics in double-giant-atom waveguide-QED systems, Phys. Rev. A **106**, 063703 (2022).
[54] Q. Bin, Y. Wu, and X.-Y. Lü, Parity-symmetry-protected multiphoton bundle emission, Phys. Rev. Lett. **127**, 073602 (2021).
[55] Q. Bin, X.-Y. Lü, F. P. Laussy, F. Nori, and Y. Wu, N-phonon bundle emission via the stokes process, Phys. Rev. Lett. **124**, 053601 (2020).
[56] S.-L. Ma, X.-K. Li, Y.-L. Ren, J.-K. Xie, and F.-L. Li, Antibunched n-photon bundles emitted by a Josephson photonic device, Phys. Rev. Res. **3**, 043020 (2021).
[57] G. C. Ménard, A. Peugeot, C. Padurariu, C. Rolland, B. Kubala, Y. Mukharsky, Z. Iftikhar, C. Altimiras, P. Roche, H. le Sueur, P. Joyez, D. Vion, D. Esteve, J. Ankerhold, and F. Portier, Emission of photon multiplets by a dc-biased superconducting circuit, Phys. Rev. X **12**, 021006 (2022).
[58] M. Uria, P. Solano, and C. Hermann-Avigliano, Deterministic generation of large Fock states, Phys. Rev. Lett. **125**, 093603 (2020).
[59] E. Sánchez-Burillo, L. Martín-Moreno, J. J. García-Ripoll, and D. Zueco, Full two-photon down-conversion of a single photon, Phys. Rev. A **94**, 053814 (2016).
[60] Y. Lu, Z. Liao, F.-L. Li, and X.-H. Wang, Integrable high-efficiency generation of three-photon entangled states by a single incident photon, Photonics Res. **10**, 389 (2022).
[61] C. Groiseau, A. E. J. Elliott, S. J. Masson, and S. Parkins, Proposal for a deterministic single-atom source of quasisuperradiant n-photon pulses, Phys. Rev. Lett. **127**, 033602 (2021).
[62] A. González-Tudela, V. Paulisch, D. E. Chang, H. J. Kimble, and J. I. Cirac, Deterministic generation of arbitrary photonic states assisted by dissipation, Phys. Rev. Lett. **115**, 163603 (2015).
[63] A. González-Tudela, V. Paulisch, H. J. Kimble, and J. I. Cirac, Efficient multiphoton generation in waveguide quantum electrodynamics, Phys. Rev. Lett. **118**, 213601 (2017).
[64] Z. Liao, X. Zeng, S.-Y. Zhu, and M. S. Zubairy, Single-photon transport through an atomic chain coupled to a one-dimensional nanophotonic waveguide, Phys. Rev. A **92**, 023806 (2015).
[65] J. D. Hood, A. Goban, A. Asenjo-Garcia, M. Lu, S.-P. Yu, D. E. Chang, and H. J. Kimble, Atom-atom interactions around the band edge of a photonic crystal waveguide, Proc. Natl. Acad. Sci. USA **113**, 10507 (2016).
[66] M.-T. Cheng, J. Xu, and G. S. Agarwal, Waveguide transport mediated by strong coupling with atoms, Phys. Rev. A **95**, 053807 (2017).
[67] J. S. Douglas, H. Habibian, C.-L. Hung, A. V. Gorshkov, H. J. Kimble, and D. E. Chang, Quantum many-body models with cold atoms coupled to photonic crystals, Nat. Photon. **9**, 326 (2015).
[68] N. V. Corzo, J. Raskop, A. Chandra, A. S. Sheremet, B. Gouraud, and J. Laurat, Waveguide-coupled single collective excitation of atomic arrays, Nature (London) **566**, 359 (2019).
[69] F. Xing, Y. Lu, and Z. Liao, Quantum correlation propagation in a waveguide-QED system with long-range interaction, Opt. Express **30**, 22963 (2022).
[70] H. Zheng, D. J. Gauthier, and H. U. Baranger, Waveguide-QED-based photonic quantum computation, Phys. Rev. Lett. **111**, 090502 (2013).
[71] P. Lodahl, S. Mahmoodian, and S. Stobbe, Interfacing single photons and single quantum dots with photonic nanostructures, Rev. Mod. Phys. **87**, 347 (2015).
[72] X. Gu, A. F. Kockum, A. Miranowicz, Y. xi Liu, and F. Nori, Microwave photonics with superconducting quantum circuits, Phys. Rep. **718-719**, 1 (2017).
[73] Z. Liao and M. S. Zubairy, Quantum state preparation by a shaped photon pulse in a one-dimensional continuum, Phys. Rev. A **98**, 023815 (2018).
[74] J. Wang, F. Sciarrino, A. Laing, and M. G. Thompson, Integrated photonic quantum technologies, Nat. Photon. **14**, 273 (2020).
[75] W. Bogaerts, D. Pérez, J. Capmany, D. A. B. Miller, J. Poon, D. Englund, F. Morichetti, and A. Melloni, Programmable photonic circuits, Nature (London) **586**, 207 (2020).
[76] J. M. Arrazola, V. Bergholm, K. Brádler, T. R. Bromley, M. J. Collins, I. Dhand, A. Fumagalli, T. Gerrits, A. Goussev, L. G. Helt, J. Hundal, T. Isacsson, R. B. Israel, J. Izaac, S. Jahangiri, R. Janik, N. Killoran, S. P. Kumar, J. Lavoie, A. E. Lita *et al.*, Quantum circuits with many photons on a programmable nanophotonic chip, Nature (London) **591**, 54 (2021).
[77] A. W. Elshaari, W. Pernice, K. Srinivasan, O. Benson, and V. Zwiller, Hybrid integrated quantum photonic circuits, Nat. Photonics **14**, 285 (2020).
[78] E. Pelucchi, G. Fagas, I. Aharonovich, D. Englund, E. Figueroa, Q. Gong, H. Hannes, J. Liu, C.-Y. Lu, N. Matsuda, J.-W. Pan, F. Schreck, F. Sciarrino, C. Silberhorn, J. Wang, and K. D. Jöns, The potential and global outlook of integrated photonics for quantum technologies, Nat. Rev. Phys. **4**, 194 (2022).
[79] Z. Liao, H. Nha, and M. S. Zubairy, Dynamical theory of single-photon transport in a one-dimensional waveguide coupled to identical and nonidentical emitters, Phys. Rev. A **94**, 053842 (2016).
[80] Z. Liao, Y. Lu, and M. S. Zubairy, Multiphoton pulses interacting with multiple emitters in a one-dimensional waveguide, Phys. Rev. A **102**, 053702 (2020).
[81] X. H. H. Zhang and H. U. Baranger, Quantum interference and complex photon statistics in waveguide QED, Phys. Rev. A **97**, 023813 (2018).
[82] M. B. Plenio and P. L. Knight, The quantum-jump approach to dissipative dynamics in quantum optics, Rev. Mod. Phys. **70**, 101 (1998).

[83] K. Mølmer, Y. Castin, and J. Dalibard, Monte Carlo wave-function method in quantum optics, J. Opt. Soc. Am. B **10**, 524 (1993).

[84] L. Scarpelli, B. Lang, F. Masia, D. M. Beggs, E. A. Muljarov, A. B. Young, R. Oulton, M. Kamp, S. Höfling, C. Schneider, and W. Langbein, 99% beta factor and directional coupling of quantum dots to fast light in photonic crystal waveguides determined by spectral imaging, Phys. Rev. B **100**, 035311 (2019).

[85] M. Mirhosseini, E. Kim, X. Zhang, A. Sipahigil, P. B. Dieterle, A. J. Keller, A. Asenjo-Garcia, D. E. Chang, and O. Painter, Cavity quantum electrodynamics with atom-like mirrors, Nature (London) **569**, 692 (2019).

[86] A. S. Sheremet, M. I. Petrov, I. V. Iorsh, A. V. Poshakinskiy, and A. N. Poddubny, Waveguide quantum electrodynamics: Collective radiance and photon-photon correlations, Rev. Mod. Phys. **95**, 015002 (2023).

[87] C. Papon, Y. Wang, R. Uppu, S. Scholz, A. D. Wieck, A. Ludwig, P. Lodahl, and L. Midolo, Independent operation of two waveguide-integrated quantum emitters, Phys. Rev. Appl. **19**, L061003 (2023).

[88] M. J. Stevens, Photon statistics, measurements, and measurements tools, in *Single-Photon Generation and Detection*, Experimental Methods in the Physical Sciences Vol. 45, edited by A. Migdall, S. V. Polyakov, J. Fan, and J. C. Bienfang (Academic Press, San Diego, 2013), Chap. 2, pp. 25–68.

[89] Y.-L. L. Fang and H. U. Baranger, Waveguide QED: Power spectra and correlations of two photons scattered off multiple distant qubits and a mirror, Phys. Rev. A **91**, 053845 (2015).